ELSEVIER

PII: S0032-3861(96)00985-8

Polymer Vol. 38 No. 16, pp. 4267–4273, 1997
© 1997 Elsevier Science Ltd
Printed in Great Britain. All rights reserved
0032-3861/97/$17.00 + 0.00

Synthesis, characterization and ionic conductivity of solid polymer electrolytes based on modified alternating maleic anhydride copolymer with oligo(oxyethylene) side chains

Liming Ding
Changchun Institute of Applied Chemistry, Chinese Academy of Sciences, Changchun 130022, China

(Received 12 August 1996; revised 29 October 1996)

Three comb polymers (CP) based on modified alternating methyl vinyl ether/maleic anhydride copolymer with oligo-oxyethylene side chains of the type $-O(CH_2CH_2O)_nCH_3$ were synthesized and characterized, and the ionic conductivity of CP/salt complexes is reported. The conductivity of these complexes was about 10^{-5}–10^{-6} S cm^{-1} at room temperature. The conductivity, which displayed non-Arrhenius behaviour, was analysed using the Vogel–Tammann–Fulcher equation. The conductivity maxima appear at lower salt concentration, when CP has longer side chains. Infrared (i.r.) was used to study the cation–polymer interaction. I.r. results also indicate that the ester in CP might decompose at 140°C and reproduce the maleic anhydride ring. © 1997 Elsevier Science Ltd.

(Keywords: solid polymer electrolytes; glass transition temperatures; ionic conductivity)

INTRODUCTION

The high ionic conductivities which have been observed in polymer/alkali metal salt complexes, particularly those involving poly(ethylene oxide) (PEO) and lithium salts, have stimulated great interest in these systems as electrolytes for solid-state, high-energy-density batteries[1,2]. The ion-conducting polymers can also be used as solvent-free electrolytes or electrode materials in sensors and electrochromic displays.

During the past 20 years, the study of solid polymer electrolytes has been very active[3,4]. PEO, the most extensively studied polymer, can form complexes with a wide range of metal salts including alkali, alkaline earth and transition metal salts. PEO/salt electrolytes suffer from one major drawback in that PEO is semicrystalline at ambient temperature. N.m.r. investigations indicate that ion transport occurs in the amorphous regions of the polymer and, taken together with temperature dependence measurements, implicate polymer segmental motion in the conduction mechanism[5]. High and valuable ionic conductivities can be obtained only after the temperature of the system exceeds the melting point of PEO, which is about 338 K. In order to destroy the crystallinity of PEO and obtain totally amorphous electrolyte materials, many researchers choose a method to prepare comb polymers by attaching short ethylene oxide (EO) unit sequences to an existing polymer backbone. Many comb polymers with oligo-oxyethylene side chains have been prepared by using polyacrylates[6–9], polyphosphazene[10–14], polysiloxane[15–19], polyglutamates[20–22] and poly(itaconic acid)[23] as the polymer backbone. These systems all show higher room temperature conductivities, when complexed with alkali metal salts, than those of PEO/salt electrolytes.

Maleic anhydride-based alternating copolymers are a group of high reactive bifunctional polymeric materials and are commercially available. Recently, Rietman and coworkers[24] have synthesized single-ion (Li) conducting polymer by reacting monomethyl ether with either poly(styrene-alt-maleic anhydride) or poly(ethylene-alt-maleic anhydride) and then treating it with LiOH solution to form lithium salt. As with other single-ion polymeric electrolytes, the room temperature conductivities of these polymers were very low (ca. 10^{-7} S cm^{-1}), and such a low level of conductivity is of no practical significance. Besides, in Rietman's work the resulting rubbery product was usually insoluble and this hindered the addition of Li ions. The present work is an alternative approach to Rietman's study, i.e., to prepare a polymer host for bi-ionic conductors by reacting monomethyl ether of PEG with another maleic anhydride alternating copolymer, poly(methyl vinyl ether-alt-maleic anhydride), and endcapping the residual carboxylic acid group with methanol. In this paper, the method of avoiding gel formation during preparation and the results of structural characterization by i.r., ^{13}C n.m.r. and elemental analysis will be reported; the ionic conductivity of CP/salt complexes was studied as a function of temperature and salt concentration.

The interaction of PEO with small molecules or ions to form complexes has been attracting wide attention since the first PEO complex (with urea) was reported in 1955[25]. Later, Liu[26] studied PEO–KI interaction by proton magnetic resonance and electrophoresis. His results indicated that K^+ interacted with the etherate oxygen of PEO. After making some proton spin-lattice relaxation time measurements, Liu and Anderson[27] indicated that the above interaction caused a reduction in segmental mobility of the polymer chain. Ibemesi and Kinsinger[28] studied the interaction of PEO with sodium tetraphenyl borate (NaTPB) by ^{13}C n.m.r. spectra and spin-lattice relaxation time (T_1). They claimed that the ion dipole interaction of PEO with inorganic salts involves the binding of the cation with etherate oxygens of the polymer, probably in a cooperative manner. In this paper, we report the preliminary results of i.r. studies on the cation–polymer interaction.

EXPERIMENTAL

Materials

Poly(methyl vinyl ether-alt-maleic anhydride) (MA), poly(ethylene-alt-maleic anhydride) (EM) and monomethylether of polyethylene glycols (PEGME) (MW 350, 550 and 750) were supplied by Aldrich Chemical Co. Ltd, and were used without further purification. *p*-Toluenesulfonic acid (PTSA, C.P. grade) was supplied by Shanghai 1st Chemical Reagent Factory, and was dried at 70°C under vacuum for 24 h prior to use. Butanone (MEK) was refluxed in the presence of C.P. grade P_2O_5 for 4 h; methanol was dried over a molecular sieve, type 4A, and then refluxed with metallic magnesium for 1 h; acetone and *n*-hexane were both refluxed with CaH_2 for 4 h. After refluxing, all the solvents were distilled just before use.

Synthesis of the comb polymer

The esterification of MA with PEGME without gel formation was achieved first by dissolving MA and PEGME (mole ratio 1/2) in freshly distilled MEK, then injecting a definite volume of MEK solution of PTSA to the mixture under a flow of N_2. The mixture was stirred continuously for 24 h at 80°C. After the reaction came to the end, the mixture was transferred to a rotary evaporator to remove MEK, then an excess amount of freshly distilled methanol (ca. 200-fold) was added to the residue so as to endcap the unreacted carboxyl group. The reaction proceeded with continuous stirring for 24 h at 60°C. The reaction mixture was then transferred to the rotary evaporator for removal of the excess methanol. Thereafter, the product (CP) was purified by reprecipitation, using distilled MEK as solvent and *n*-hexane as precipitant. Generally, four reprecipitations were necessary.

All three polymers present themselves as white elastomeric solids. The polymers that we designate as CP350, CP550 and CP750 were prepared by using PEGME, $HO(CH_2CH_2O)_nCH_3$, with different molecular weights of 350, 550 and 750; $n = \langle 7 \rangle$, $\langle 12 \rangle$ and $\langle 17 \rangle$ respectively, the angle brackets indicating that this is an average value.

General methods

Absorbance i.r. spectra were obtained on a BIO-RAD FTS-7 spectrometer. Samples for i.r. spectroscopy were cast onto KBr plates. A Varian unity-400 spectrometer was used to obtain the ^{13}C n.m.r. spectra of CP and three model polymers, poly(ethylene-alt-maleic anhydride)(EM), poly(methyl vinyl ether-alt-maleic anhydride) (MA) and dimethyl ester of MA (MM). Elemental analysis was performed with a Model 1106 Elemental Analyzer provided by Carlo Erba Strumentazione Co. Anal. calcd for $C_{23}H_{42}O_{12}$ per repeat unit of CP350: C, 54.11; H, 8.29. Found: C, 54.14; H, 8.32. Anal. calcd for $C_{33}H_{62}O_{17}$ per repeat unit of CP550: C, 54.23; H, 8.55. Found: C, 54.28; H, 8.49. Anal. calcd for $C_{43}H_{82}O_{22}$ per repeat unit of CP750: C, 54.30; H, 8.69. Found: C, 54.39; H, 8.73. D.s.c. measurements were performed on a Perkin–Elmer DSC-7 instrument equipped with a liquid nitrogen cooling system and a heating/cooling rate of 20 K min^{-1}. Polymer complexes were hermetically sealed in aluminium pans. The samples were subjected to a heating–cooling–reheating cycle and the temperature range used was generally −70 to 135°C. The glass transition temperatures (T_g) were determined as the midpoints of the heat capacity change during the relaxation temperature.

Preparation of solid electrolyte film

Anhydrous $LiClO_4$ and $LiCF_3SO_3$ (Aldrich) were dried under reduced pressure (10^{-3} torr) at 130°C for 24 h and were then dissolved in dry acetone. CP/acetone and salt/acetone were mixed in appropriate proportions to obtain polymer/salt complexes of the desired composition. The solutions were cast on Teflon dishes, and acetone was allowed to evaporate at room temperature under a nitrogen stream until the solutions did not flow. The samples obtained were dried thoroughly *in vacuo* at 70°C for 72 h until the water content, determined by using Karl Fischer reagent, was less than 0.01%. Dried samples were stored in sealed containers within an argon-filled dry box. All samples were dried again overnight in a vacuum at 70°C before conductivity measurements were made.

Conductivity measurements

Polymer electrolyte samples of 1 cm diameter and approximately 0.025 cm thickness were placed between two spring-loaded stainless steel electrodes. Conductivity measurements were carried out in a thermally insulated box using a fast flowing stream of dry nitrogen to maintain the required temperature. Thermocouples positioned close to the samples were used to monitor and control the temperature of the electrolyte films to an accuracy of better than ±0.5 K. The complex impedence of the samples was measured in the 298–373 K temperature range, with a Solartron 1255 FRA connected to a Solartron 1287 electrochemical interface; the applied signal amplitude was 1 V in the nominal frequency range of 0.1 Hz to 1 MHz. The conductivity was determined as a function of temperature, allowing an equilibration time of 1 h at each incremental rise in temperature.

RESULTS AND DISCUSSION

Scheme 1 summarizes the synthetic route for the comb-like polymer host based on maleic anhydride copolymer backbone. Under the catalytic action of externally added acid, the esterification of the alternating maleic anhydride copolymer with low MW alcohol can only form a semi-ester; i.e., only one of the two carboxylic acids can be converted into ester[29]. In our case, using

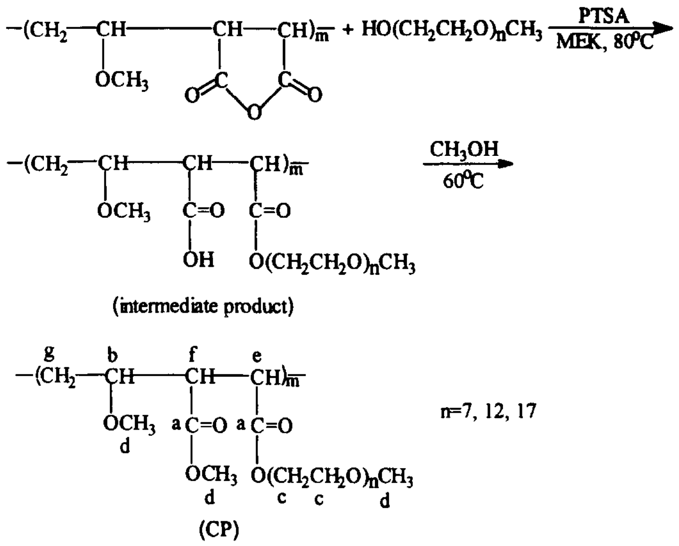

Scheme 1 Synthesis of CP

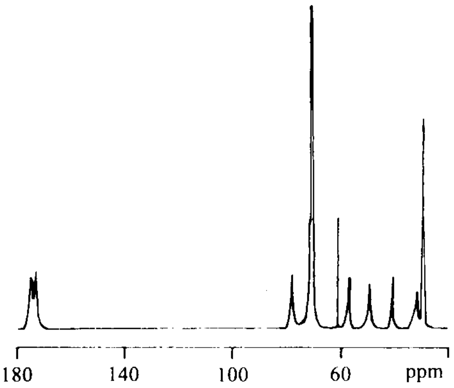

Figure 1 ^{13}C n.m.r. spectrum for CP750

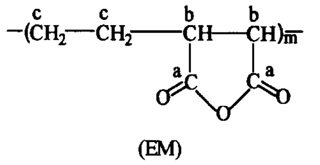

Scheme 2 Structure of EM

PEGME as an esterification agent, a similar result was obtained. The same result was also reported by Rietman[24]. However, in contrast to the low MW monofunctional alcohol, the use of PEGME often results in an insoluble product. The formation of the insoluble product would bring about many difficulties in the experimental work, e.g., purification, characterization and film formation. Gel formation might be caused by the presence of trace impurity of unmethylated PEG, which is very difficult to remove completely from the bulk of PEGME. We therefore tried to overcome this difficulty by allowing the esterification to proceed in solution, and have succeeded in obtaining completely soluble products. Several organic solvents such as DMF, cyclohexanone and MEK have been selected for solution esterification. Among them, MEK seemed to be the most favourable. Although DMF is a good solvent for MA, it usually causes the product to discolour; as for cyclohexanone, the solubility of the intermediary is rather poor. THF also manifests itself as a fairly good solvent for this esterification. During synthesis, it was found that after the completion of the first step of the reaction, the intermediary was very difficult to obtain since it readily became an insoluble gel even if it was dried in an oven at 50°C. Thus the second step of the reaction was started by adding an excess amount of methanol directly after the removal of MEK. Only in this way could a completely soluble final product CP be acquired.

In the i.r. spectrum of the purified final product CP350, both the absorption peaks at 1857.8 and 1779.2 cm^{-1} are absent, indicating that the anhydride has been converted completely. The strong absorptions at 1732.4 and 1101.8 cm^{-1} show that the product is a polyester of poly(ethylene glycol).

The structure of CP was further examined by ^{13}C n.m.r. spectrum. According to the presumed formula of CP (see *Scheme 1*), there are four different carbons in the main chain, i.e. one methylene carbon **g** and three tertiary carbons **b**, **e**, **f**. In the side chains, there are two carbonyl carbons **a**, three methyl carbons **d**, one of which belongs to the methoxyl group and the other two to the ester groups, and the methylene carbons **c** in the PEG group. The ^{13}C n.m.r. spectrum of CP750 is shown in *Figure 1*. In order to judge which signal represents its corresponding carbon in CP, it is first necessary to study the ^{13}C n.m.r. spectra of model polymers (EM, MA and MM) which are analogous to CP.

Except for the solvent peaks, the ^{13}C n.m.r. spectrum of EM (*Scheme 2*) exhibits only three sets of doublet signals. The splitting of the peaks is due to the difference in stereo-configuration for the anhydride group. From low to high field, we assign 175.6–173.4 ppm to the carboxyl carbons **a**; 47.8–45.8 ppm to the tertiary carbons **b**; and 27.3–25.9 ppm to the secondary carbons **c**. The assignment was based on the disappearance of the signals of the quaternary carbons **a** in the carboxyl group and the inversion of the signals of the secondary carbons **c** in the methylene group in the DEPT spectrum of EM.

From the formula of MA as shown below, the methoxyl group definitely complicates the chain structure of the copolymer and increases the number and splitting of the signal. The presence of $-OCH_3$ would

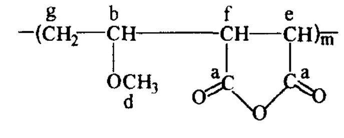

(MA)

Scheme 3 Structure of MA

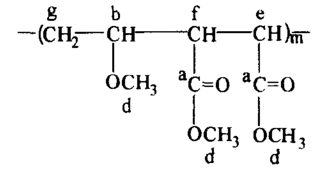

(MM)

Scheme 4 Structure of MM

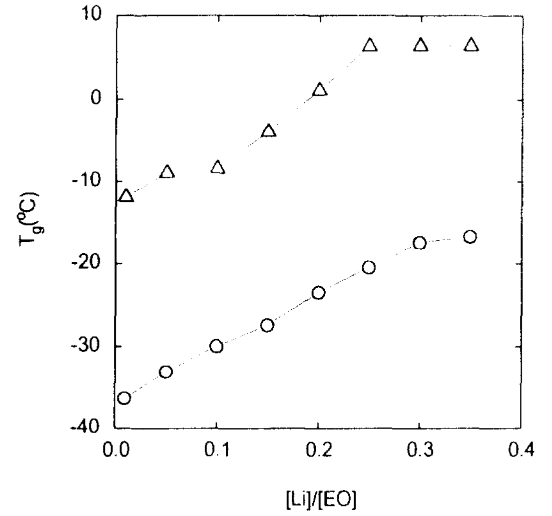

Figure 2 Variation of glass transition temperature with salt concentration for CP350/LiClO$_4$ complexes: T_{g1} (○), T_{g2} (△)

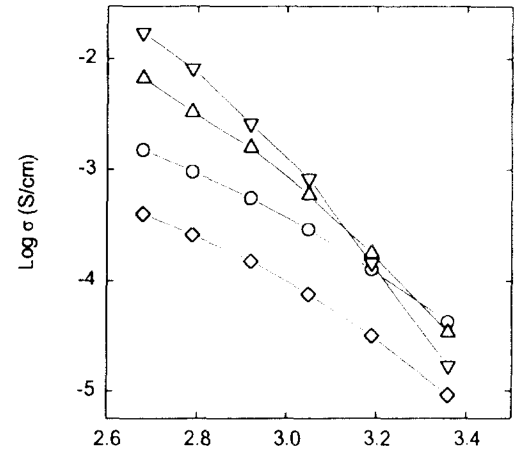

Figure 3 Plots of logσ vs 1000/T for CP350/LiClO$_4$ complexes: [Li]/[EO] = 0.01 (◇); 0.05 (○); 0.10 (△); 0.20 (▽)

shift the signals of tertiary carbon **b** and adjacent secondary carbon **g** to low field. The carbon in the methyl group of aliphatic methyl ether is usually situated around 57 ppm[30], so from low to high field the signals in the ^{13}C n.m.r. spectrum of MA (*Scheme 3*) can be assigned as follows: **a**, quaternary carbon in the carboxyl group of maleic anhydride, 173.7–170.9 ppm; **b**, tertiary carbon, 78.8–77.9 ppm; **d**, primary carbon in the methoxyl group, 59.2–57.4 ppm; **e**, tertiary carbon, 51.6–48.4 ppm; **f**, tertiary carbon, 41.1–37.8 ppm; and **g**, secondary carbon in the methylene group, 34.5–31.3 ppm.

For the model polymer dimethyl ester of poly(vinyl methyl ether-alt-maleic anhydride) (MM), its formula is shown below. From the assignment of the signals to carbons of the model polymers discussed above and the DEPT spectrum of MM, signals in the ^{13}C n.m.r. spectrum of MM (*Scheme 4*) can be assigned as follows: **a**, quaternary carbon in the carboxyl group, 175.0–172.8 ppm; **b**, tertiary carbon of methine group, 78.2–77.2 ppm; **d**, methoxyl and methyl ester carbon, 58.4–56.6 ppm; **e**, methine carbon, 49.6–49.0 ppm; **f**, methine carbon, 41.4–40.4 ppm; and **g**, secondary carbon of the methylene group, 31.9–31.6 ppm.

The ^{13}C n.m.r. spectrum of CP750 shown in *Figure 1* is quite similar to that of MM, except for two additional signals situated at 72.8–69.9 ppm and 61.2 ppm. Apparently the former is the concentration of the secondary carbon **c** in the –(CH$_2$CH$_2$O)– group, while the latter is due to the carbon in the –CH$_2$OH group which arises from the unreacted end of PEG mixed with PEGME. Therefore, the assignment of the signals in *Figure 1* is: carbon **a**, 175.8–172.5; **b**, 78.2–77.2; **c**, 72.8–69.9; **d**, 57.5; **e**, 49.6; **f**, 41.1; and **g**, 32.1 ppm. On the basis of the above characterization results, the presumed structure of CP shown in *Scheme 1* is now well confirmed.

In order to clarify the relationship between ionic conductivity and segmental motion of the polymer matrix, the dependence of T_g on salt content should be determined. CP350/LiClO$_4$ complexes showed only glass transitions in d.s.c. curves, which indicated that these samples were completely amorphous at ambient temperatures. It is very interesting to note that there are two glass transitions, and that the two T_gs increase with increasing [Li]/[EO] ratio (as shown in *Figure 2*). T_{g1} and T_{g2} can be attributed to the glass transition temperature of oligo-oxyethylene side chains and polymer backbone respectively, since the side chains are more flexible than the –C–C–C–C– backbone. At low salt concentrations, the large value of ΔT_g indicates a substantial dissociation of the salt to form solvated cations, leading to crosslinking or chain stiffening, whereas low ΔT_g values suggest that the dissociation is small and the salt exists predominantly as ion pairs[23]. There are two factors involved in the increase of T_g with salt content: (1) interaction between ether oxygen atoms and Li$^+$ increases the microviscosity of the solid electrolyte film; and (2) the polymer segment is expanded by the introduction of charges on the polymer chains because of the electrostatic repulsion[31]. If the –COO(CH$_2$CH$_2$O)$_n$CH$_3$ groups in CP are defined as the side chains, the remaining backbone still consists of polar groups, i.e., –OCH$_3$, –COOCH$_3$, which can also interact with Li$^+$ effectively; thus T_{g2} increases with the increase of salt content. This contrasts finely with Watanabe's work[15] in which the T_g of the siloxane backbone remained unchanged owing to the absence of polar groups attaching to the remaining backbone.

The temperature dependence of the ionic conductivity of CP350/LiClO$_4$ electrolyte films is shown in *Figure 3* over a range of salt concentrations. These data were

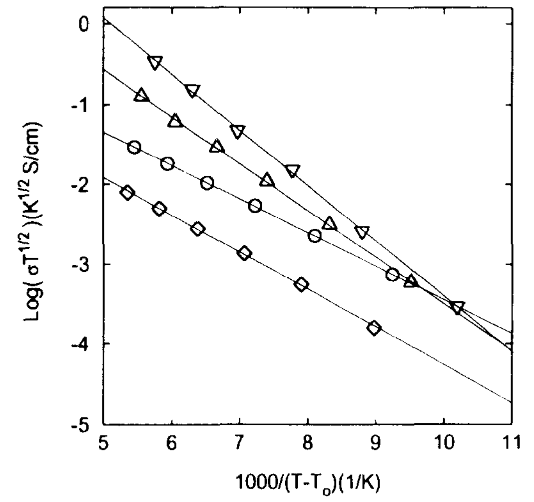

Figure 4 Plots according to the VTF equation: [Li]/[EO] = 0.01 (◇); 0.05 (○); 0.10 (△); 0.20 (▽)

Table 1 Parameters for the CP350/LiClO$_4$ complexes derived from the VTF equation

No.	[Li]/[EO]	A	B
1	0.01	2.7	1082
2	0.05	6.1	976
3	0.10	240	1354
4	0.20	3548	1601

collected on heating, and the discrepancies with the corresponding cooling curves were generally less than 5%. The curvature of the plots suggests non-Arrhenius behaviour, which was first observed for PEO/salt and PPO/salt complexes and described by the Vogel–Tammann–Fulcher (VTF) equation[32–34]:

$$\sigma = AT^{-1/2}\exp[-B/(T - T_0)] \qquad (1)$$

where A is a pre-exponential term related to the concentration of the free charge carriers, B is pseudo-activation energy which is directly proportional to the free energy barrier, and T_0 can be regarded as the temperature below which there is no further entropy loss due to configurational changes in the polymer. The VTF plots of CP350/LiClO$_4$ complexes show excellent linearity (*Figure 4*) when taking T_0 as $T_{gl} - 50$ K. The values of A and B listed in *Table 1* are determined by the use of a computer-fitting technique.

The salt concentration dependence of ionic conductivity can be easily illustrated by examining isothermal plots of the log (conductivity) vs [Li]/[EO] ratios, as shown in *Figure 5*. At 25, 55 and 85°C, three pronounced conductivity maxima, i.e. 4.9×10^{-5}, 1.7×10^{-3} and 8.13×10^{-3} S cm^{-1} at [Li]/[EO] ratios of 0.064, 0.15 and 0.19 respectively can be observed. The conductivity data pass through a maximum, indicating that the effects of increasing charge carrier density are overcome by the accompanying decrease in segmental mobility, increase in the formation of ion triplets and multiple-ion aggregates, increase in the charge cloud effects retarding ion transport, and drop in the salt ionization at higher concentrations[9,35]. The decrease in segmental mobility arises from virtual crosslinking and has an obvious signature in the increased glass transition temperatures[19].

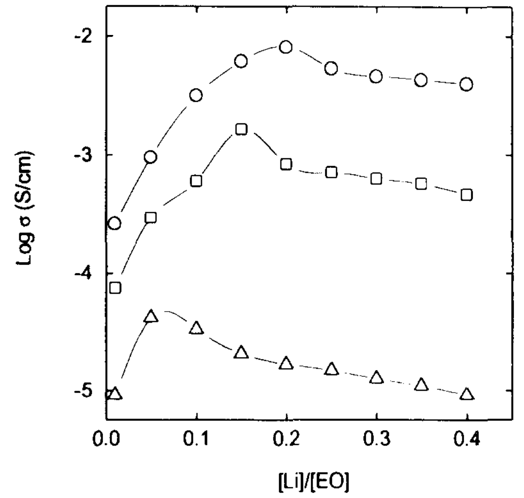

Figure 5 Variation of log σ with salt content for CP350/LiClO$_4$ complexes: 298 K (△), 328 K (□) and 358 K (○)

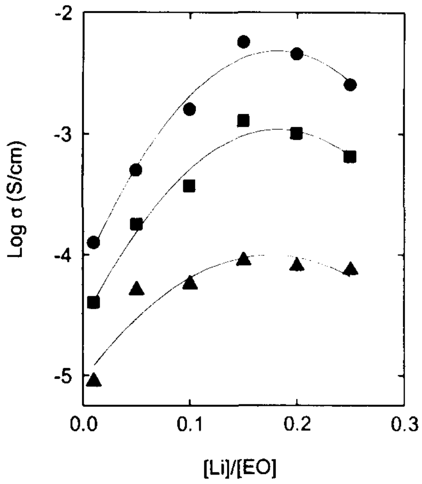

Figure 6 Variation of log σ for CP350/LiClO$_4$ complexes with salt concentration, but measured at constant values of $(T - T_{gl})$ of 60 K (▲), 80 K (■) and 100 K (●)

The free volume model is very useful for discussing the ion transport mechanism and for understanding the polymer segment mobility. It states that as temperature increases, the expansivity of the material produces local empty space, free volume, into which ions, solvated molecules or polymer segments themselves can move[5]. The overall mobility of the material is determined by the amount of free volume present in the material. As temperature increases, the amount of free volume increases, leading to increases of ion mobility and segment mobility. Only at higher salt concentrations can the negative effect on ionic conductivity resulting from stiffening of the coordinated side chains, the formation of ion triplets, aggregates and charge cloud effects counteract the positive effect on conductivity resulting from the increase of the overall mobility of the electrolyte material. Therefore, the conductivity maximum moves to a higher salt concentration as the temperature increases. When we replot the data at constant chain flexibility, as shown in *Figure 6*, where log σ is presented as a function of constant $(T - T_{gl})$ values, the conductivity maxima are observed at a constant [Li]/[EO] ratio of approximately 0.18. This method eliminates the effect of T_g on conductivity by

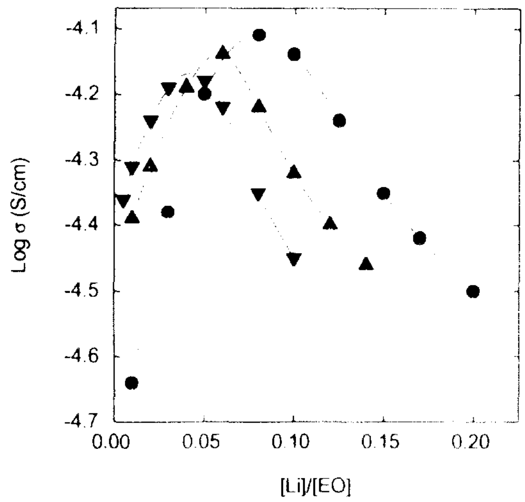

Figure 7 $LiCF_3SO_3$ salt content dependence of ionic conductivity for CP350 (●), CP550 (▲) and CP750 (▼) complexes at 25°C

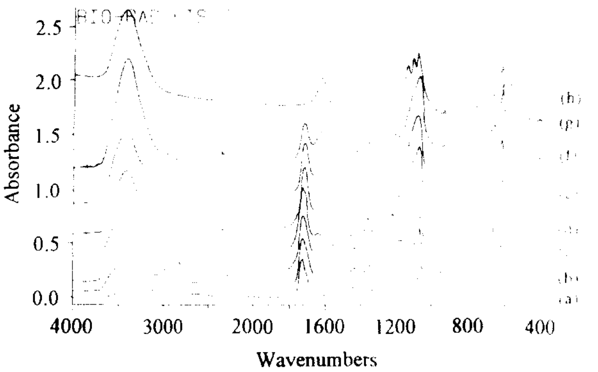

Figure 8 I.r. spectra for pure CP550 (a), $LiClO_4$ (h) and CP550/$LiClO_4$ complexes with [Li]/[EO] ratios of 0.01 (b), 0.1 (c), 0.2 (d), 0.3 (e), 0.4 (f) and 1.0 (g)

comparing conductivities at different salt concentrations but at a constant temperature above the T_g of each polymer/salt system as first proposed by Cowie and Martin[8]. The result proves again that the increase of T_g is partly responsible for the decrease of conductivity[9].

Figure 7 shows the effect of length of side chains on ionic conductivity. The conductivity maximum appears at lower salt concentrations when CP has longer side chains. This may be due to the greater increase of microviscosity with salt content for CP/salt systems with longer side chains. Also, the stronger interchain interactions between longer side chains by the crosslinking effect of the added lithium cations would further increase the microviscosity, which has the greatest effect on ionic mobility[36]. *Figure 7* also shows that CP/$LiCF_3SO_3$ electrolyte with longer side chains exhibits a higher ionic conductivity at low salt concentrations. It suggests that the stronger interaction between the longer side chains and Li^+ promotes the dissociation of $LiCF_3SO_3$[37].

The ionic conductivity of solid polymer electrolytes is controlled by the mobility of side chains, ion–dipole interaction and the structure of complexes. So it is very important to study the cation–polymer interaction and get enough structural information for us to study the ion transport mechanism. Shriver *et al.*[38,39] and Torell and Schantz (ref. 4, p. 1). have focused their attention on the structure of PEO/salt and PPO/salt complexes. They have studied cation–polymer interactions extensively by i.r. and Raman techniques and obtained satisfactory results. In our vibrational study of the CP550/$LiClO_4$ complexes, the main interest is focused on the changes of C–O–C vibrational modes. All CP550/$LiClO_4$ complexes have very similar i.r. spectra (as shown in *Figure 8*). When compared with pure CP550, some obvious differences can be found. Some slight shifting to lower wavenumber and broadening of the 1101.8 cm^{-1} band does occur (see *Table 2*). This may be due to the coordination of Li^+ to ether oxygens. The new band at 624.8 cm^{-1} of medium intensity in *Figure 8b* is characteristic of ClO_4^-. This band also shifts to lower wavenumber because of the coordination, but this shifting is slighter than that of the C–O–C band.

Table 2 Bands of C–O–C and ClO_4^- in the i.r. spectra (cm^{-1})

[Li]/[EO]	C–O–C	ClO_4
0	1101.8	
0.01	1100.0	624.8
0.1	1091.6	625.0
0.2	1090.8	625.7
0.3	1077.0	624.9
0.4	1080.9	625.5
1.0	1078.3	625.3
$LiClO_4$		627.3

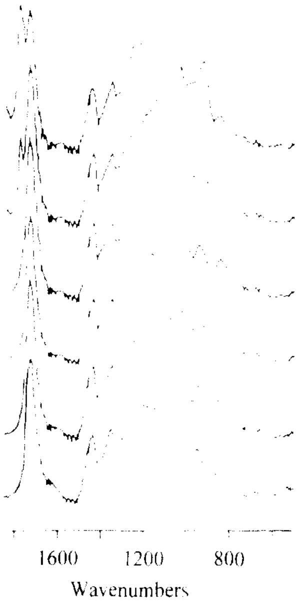

Figure 9 I.r. spectra for CP350 at various temperatures

In order to understand the thermal stability of CP and ascertain the mechanism of thermal decomposition, we tried to inspect the molecular structure change of CP350 during the gradual temperature-raising process by using a temperature-changing i.r. technique with a heating rate of 2°C min^{-1}. *Figure 9* shows that the structure of CP350 does not change until the temperature reaches 140°C, when two new absorbance peaks appear at 1859.5 and 1781.2 cm^{-1}. The new bands are very characteristic of a maleic anhydride ring. This implies that the ester in CP350 might decompose at 140°C and reproduce the maleic anhydride ring (as shown in *Scheme 5*). So the upper-limit temperature of the CP/salt complexes as practical solid electrolyte materials might be 140°C.

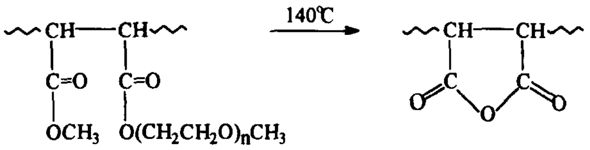

Scheme 5 Thermal decomposition of CP

CONCLUSIONS

Three new amorphous comb polymers with low T_g values have been synthesized on the basis of alternating maleic anhydride copolymer. They can form single-phase amorphous complexes with alkali metal salts which display high ionic conductivities at ambient temperatures. The temperature dependence of the ionic conductivity suggests that the conduction follows the WLF mechanism, which is confirmed by Vogel–Tammann–Fulcher plots. Thus the ionic conductivity of these polymer electrolytes is strongly affected by segmental motion in the polymer matrix. In addition, the complexes are soluble and can readily be cast into dimensionally stable, free-standing thin films, which suggests that they are viable alternatives for low-temperature thin-film battery applications. Further electrochemical studies on these rubbery electrolytes are in progress.

REFERENCES

1. Fenton, D. E., Parker, J. M. and Wright, P. V., *Polymer*, 1973, **14**, 589.
2. Armand, M. B., Chabagno, J. M. and Duclot, M., in *Fast Ion Transport in Solids*, ed. P. Vashishita, J. N. Mundy and G. K. Shenoy. North-Holland, Amsterdam, 1979, p. 131.
3. MacCallum, J. R. and Vincent, C. A. (ed.), *Polymer Electrolytes Reviews—I*. Elsevier Applied Science, London, 1987.
4. MacCallum, J. R. and Vincent, C. A. (ed.), *Polymer Electrolytes Reviews—II*. Elsevier Applied Science, London, 1989.
5. Ratner, M. A. and Shriver, D. F., *Chem. Rev.*, 1988, **88**, 109.
6. Bannister, D. J., Davies, G. R., Ward, I. M. and McIntyre, J. E., *Polymer*, 1984, **25**, 1291.
7. Cowie, J. M. G. and Martin, A. C. S., *Polym. Commun.*, 1985, **26**, 298.
8. Cowie, J. M. G. and Martin, A. C. S., *Polymer*, 1987, **28**, 627.
9. Cowie, J. M. G., Martin, A. C. S. and Firth, A.-H., *Br. Polym. J.*, 1988, **20**, 247.
10. Cowie, J. M. G. and Sadaghianzadeh, K., *Makromol. Chem., Rapid Commun.*, 1989, **9**, 387.
11. Blonsky, P. M., Shriver, D. F., Austin, P. E. and Allcock, H. R., *J. Am. Chem. Soc.*, 1984, **106**, 6854.
12. Allcock, H. R., Austin, P. E., Neenan, T. X., Sisko, J. T., Blonsky, P. M. and Shriver, D. F., *Macromolecules*, 1986, **19**, 1508.
13. Ganabathiappan, S., Chen, K. and Shriver, D. F., *Macromolecules*, 1988, **21**, 2301.
14. Lerner, M. M., Tipton, A. L., Shriver, D. F., Dembek, A. A. and Allcock, H. R., *Chem. Mater.*, 1991, **3**, 1117.
15. Watanabe, M., Nagano, S., Sanui, K. and Ogata, N., *J. Power Sources*, 1987, **20**, 327.
16. Hall, P. G., Davies, G. R., McIntyre, J. E., Ward, I. M., Bannister, D. J. and Le Brocq, K. M. F., *Polym. Commun.*, 1986, **27**, 98.
17. Fish, D., Khan, I. M., Wu, E. and Smid, J., *Br. Polym. J.*, 1988, **20**, 281.
18. Zhou, G., Khan, I. M. and Smid, J., *Polym. Commun.*, 1989, **30**, 52.
19. Lonergan, M. C., Ratner, M. A. and Shriver, D. F., *J. Am. Chem. Soc.*, 1995, **117**, 2344.
20. Watanabe, M. and Ogata, N., *Br. Polym. J.*, 1988, **20**, 181.
21. Yamaguchi, Y., Aoki, S., Watanabe, M., Sanui, K. and Ogata, N., *Solid State Ionics*, 1990, **40/41**, 628.
22. Watanabe, M., Aoki, S., Sanui, K. and Ogata, N., *Polym. Adv. Techn.*, 1993, **4**, 179.
23. Cowie, J. M. G., Ferguson, R. and Martin, A. C. S., *Polym. Commun.*, 1987, **28**, 130.
24. Rietman, E. A. and Kaplan, M. L., *J. Polym. Sci., Part C, Polym. Lett.*, 1990, **28**, 187.
25. Baker, G. E. and Ranauto, H. T., *J. Am. Oil Chem. Soc.*, 1955, **32**, 249.
26. Liu, K. J., *Macromolecules*, 1968, **1**, 308.
27. Liu, K. J. and Anderson, J. E., *Macromolecules*, 1969, **2**, 235.
28. Ibemesi, J. A. and Kinsinger, J. B., *J. Polym. Sci.*, 1980, **18**, 1123.
29. Ratzsch, M., *Prog. Polym. Sci.*, 1988, **13**, 277.
30. Silverstein, R. M., Bassler, G. C. and Morrill, T. C., in *Spectrometric Identification of Organic Compounds*, 4th edn. John Wiley & Sons, New York, 1981.
31. Tsuchida, E., Kobayashi, N. and Ohno, H., *Macromolecules*, 1988, **21**, 96.
32. Vogel, H., *Phys. Z.*, 1921, **22**, 645.
33. Tammann, V. G. and Hesse, W., *Z. Anorg. Allg. Chem.*, 1926, **156**, 245.
34. Fulcher, G. S., *J. Am. Ceram. Soc.*, 1925, **8**, 339.
35. Cowie, J. M. G. and Sadaghianizadeh, K., *Polymer*, 1989, **30**, 509.
36. Tsuchida, E., *J. Macromol. Sci.-Chem.*, 1988, **A25**, 687.
37. Kobayashi, N., Uchiyama, M., Shigehara, K. and Tsuchida, E., *J. Phys. Chem.*, 1985, **89**, 987.
38. Papke, B. L., Ratner, M. A. and Shriver, D. F., *J. Phys. Chem. Solids*, 1981, **42**, 493.
39. Dupon, R., Papke, B. L., Ratner, M. A., Whitmore, D. H. and Shriver, D. F., *J. Am. Chem. Soc.*, 1982, **104**, 6247.